

**PERIODIC BURIED OBJECT APPROACH FOR  
SOLVING SCATTERING PROBLEMS RELATED  
TO PERIODIC ROUGH SURFACES**

**M.Sc Thesis by  
Selda YILDIZ, B.Sc.**

**Department : ELECTRONICS AND COMMUNICATION ENGINEERING  
Programme : TELECOMMUNICATION ENGINEERING**

**JUNE 2008**

**PERIODIC BURIED OBJECT APPROACH FOR  
SOLVING SCATTERING PROBLEMS RELATED TO  
PERIODIC ROUGH SURFACES**

**M.SC. Thesis by  
Selda YILDIZ, B.Sc.  
(504061336)**

**Date of submission : 5 May 2008**

**Date of defence examination: 11 June 2008**

**Supervisor (Chairman): Prof. Dr. İbrahim AKDUMAN (İTÜ)**

**Members of the Examining Committee Assoc. Prof.Dr. Ali YAPAR (İTÜ)**

**Assist. Prof.Dr. Lale Tükenmez ERGENE  
(İTÜ)**

**JUNE 2008**

**ENGEBELİ PERİYODİK YÜZEYLERDEN SAÇILMA  
PROBLEMLERİNİN ÇÖZÜMÜ İÇİN PERİYODİK  
GÖMÜLÜ CİSİM YAKLAŞIMI**

**YÜKSEK LİSANS TEZİ  
Müh. Selda YILDIZ  
(504061336)**

**Tezin Enstitüye Verildiği Tarih : 5 Mayıs 2008**

**Tezin Savunulduğu Tarih : 11 Haziran 2008**

**Tez Danışmanı : Prof. Dr. İbrahim AKDUMAN (İTÜ)  
Diğer Jüri Üyeleri Doç. Dr. Ali YAPAR (İTÜ)  
Yar. Doç. Dr. Lale Tükenmez ERGENE (İTÜ)**

**HAZİRAN 2008**

## ACKNOWLEDGEMENTS

There are several people I wish to thank for the precious support they provided to my research during this study, which contributed to my personal and professional development.

First and foremost, I would like to thank my advisor Prof. İbrahim Akduman having gave me the opportunity to join his group and the inspiration of doing research in an exciting project with both theoretical and experimental aspects. Since I begun working as an undergraduate, he supported me with his deep knowledge and patience, provided me unflinching encouragement in various ways, and taught me to how to behave in a team. I am grateful to Prof. Akduman, who anyone hopes to meet in his life, for having shown me how all those qualities can coexist in a single person.

I want to offer my sincerest gratitude to Assoc. Prof Ali Yapar for his supervision, precious guidance, advice, and support throughout this study. His truly scientist intuition has inspired my growth as a student.

I would also like to express my gratitude to Dr. Yasemin Altuncu who not only guided me throughout this research, but also helped me improve my perspective about the subject.

I also owe my thanks to TUBITAK for the support during my master education and thanks to Electromagnetic Research Group at ITU for their support in every step of this research.

Also, thanks to my roommate and office mate Çağla and roommate Özlem for their support and encouragement.

A special thank goes to my friend Yasemin Demir. This paper would not have been possible without her endless support and encouragement that was always by my side. I also gratefully thank Jesse Howell for his continuous support, and help with the reviewing the paper. Many thanks for Başak, Sami and Eda. The burden of writing this thesis was lessened by the support and humor of all these lovely friends.

Lastly, and most importantly, I am eternally grateful to my parents that bore me, raised me, taught me, supported me, and loved me. I am sincerely thankful to my brothers and

sisters for their support and encouragement in various ways throughout all my studies.  
To my family I dedicate this thesis.

June, 2008

Selda Yıldız

## TABLE OF CONTENT

<b>ABBREVIATIONS</b>	<b>IV</b>
<b>LIST OF FIGURES</b>	<b>V</b>
<b>LIST OF SYMBOLS</b>	<b>VI</b>
<b>SUMMARY</b>	<b>VII</b>
<b>ÖZET</b>	<b>VIII</b>
<b>1. INTRODUCTION</b>	<b>1</b>
<b>2. FORMULATION OF THE PROBLEM</b>	<b>4</b>
2.1. Geometry of the Problem	4
2.2. The Floquet Theorem	5
<b>3. PERIODIC OBJECT MODELLING</b>	<b>10</b>
3.1. Buried Object Approach	10
3.2. Periodic Buried Object Approach Modelling	11
<b>4. A MOMENT OF METHOD SOLUTION</b>	<b>15</b>
<b>5. NUMERICAL IMPLEMENTATION</b>	<b>18</b>
5.1. Sinusoidally Periodic Surface	18
5.2. Periodic Random Surface	21
5.3. The Effect of the Roughness on the Propagation of Incident Plane wave	22
5.4. Locally Rough Surface	25
<b>5. CONCLUSIONS</b>	<b>30</b>
<b>REFERENCES</b>	<b>31</b>
<b>BIOGRAPHY</b>	<b>34</b>

## **LIST OF ABBREVIATIONS**

<b>MoM</b>	: Method of Moment Solution
<b>BOA</b>	: Buried Object Approximation
<b>PBOA</b>	: Periodic Buried Object Approximation
<b>RMSE</b>	: Root Mean Square Error

## LIST OF FIGURES

	<u>Sayfa No</u>
<b>Figure 2.1</b> : Geometry of the problem.....	5
<b>Figure 2.2</b> : Periodic structures.....	6
<b>Figure 3.1</b> : Buried object modeling of the rough surface.....	12
<b>Figure 5.1</b> : Sinusoidally rough surface profile.....	19
<b>Figure 5.2</b> : Comparison of the amplitude and the phase of the scattered field obtained by Analytical and PBOA methods for the surface given in (5.1).....	20
<b>Figure 5.3</b> : Comparison of the amplitude and the phase of the scattered field obtained by Analytical and PBOA methods for the surface given in (5.2) .....	20
<b>Figure 5.4</b> : Comparison of the amplitude and the phase of the scattered field obtained by Perturbation and PBOA methods for the random surface of $h = 0.006\lambda, \ell = 0.6\lambda$ and $L = 4\lambda$ .....	21
<b>Figure 5.5</b> : Variation of the total field amplitude in a rectangular region for the random periodic surface of $h = 0.2\lambda, \ell = 0.8\lambda$ and $L = 10\lambda$ .....	22
<b>Figure 5.6</b> : Variation of the total field amplitude in a rectangular region for the random periodic surface of $h = 0.08\lambda, \ell = 0.8\lambda$ and $L = 10\lambda$ .....	23
<b>Figure 5.7</b> : Variation of the total field amplitude for the random periodic air-micra interface with $h = 0.15\lambda, \ell = 0.6\lambda, L = 11\lambda$ and $\phi_0 = \pi/2$ ....	24
<b>Figure 5.8</b> : Variation of the total field amplitude for the random periodic air micra interface with $h = 0.15\lambda, \ell = 0.6\lambda, L = 11\lambda$ and $\phi_0 = \pi/4$ .....	24
<b>Figure 5.9</b> : <b>(a)</b> A locally rough surface interface of infinite extend <b>(b)</b> it periodic model .....	26
<b>Figure 5.10</b> : Comparison of the amplitude and the phase of the scattered field obtained by BOA and PBOA for a locally rough surface given in (5.3).....	27
<b>Figure 5.11</b> : RMSE between BOA and PBOA for the surface given in (5.3)....	27
<b>Figure 5.12</b> : Comparison of the amplitude and the phase of the scattered field obtained by BOA and PBOA methods for a random surface of $h = 0.4\lambda, \ell = 0.7\lambda$ and .....	28
<b>Figure 5.13</b> : RMSE between BOA and PBOA for a random surface of $h = 0.4\lambda, \ell = 0.7\lambda$ and $\ell_R = 4\lambda$ .....	29



## LIST OF SYMBOLS

$L$	: Period of the surface
$\Gamma_0$	: Surface
$h$	: Maximum peak point of the surface
$\ell$	: Correlation length
$\epsilon_0$	: Dielectric permittivity of the free space
$\mu_0$	: Magnetic permeability of the free space
$\epsilon_1, \epsilon_2,$	: Relative dielectric permittivities of the first and second media, respectively.
$\sigma_1, \sigma_2,$	: Conductivities of first and second media, respectively.
$\Gamma_0$	: Surface
$E_i$	: Incident electric field
$E_t$	: Total electric field
$u_i$	: A time-harmonic plane wave
$u$	: Total field
$\beta_1, \gamma_1, \gamma_2$	: Propagation constants
$k_1, k_2,$	: Wave number of the first and second media, respectively.
$\Phi_0$	: Incidence angle
$\omega$	: Angular frequency
$u_0$	: Total electric field in a single period in the case of the interface is flat
$R_{12}$	: Reflection coefficient
$T_{12}$	: Transmission coefficient
$B_n$	: Regions in a period
$N$	: Number of the cylindrical bodies in a period
$G_p$	: Periodic Green's function of the two half spaces media
$P$	: Value of truncation numer
$v_n$	: Object function
$\delta$	: Dirac delta distribution
$K$	: A linear operator
$M_n$	: Number of the small cells in one region $B_n$
$S_{nm}$	: $m$ 'th cell of the region $B_n$
$y^{nm}$	: Center point of the cell $S_{nm}$
$C^{nm}$	: Coefficients for the calculation of $G_p$
$a$	: Radius of a circular cell
$\lambda$	: Wave length
$\ell_R$	: Roughness length

## **PERIODIC BURIED OBJECT APPROACH FOR SOLVING SCATTERING PROBLEMS RELATED TO PERIODIC ROUGH SURFACES**

### **SUMMARY**

In this study, a new approach for the scattering of electromagnetic waves from periodic dielectric rough surfaces is addressed. The method is an extension of the buried object approach (BOA) which is an efficient method for the scattering of electromagnetic waves from dielectric rough surfaces of infinite extent. The basic idea in the Periodic Buried Object Approach (PBOA) is to assume the fluctuations of the rough surface from the flat one as buried objects in a periodic two half - spaces medium with planar interface. Such an approach allows formulating the problem as a scattering of electromagnetic waves from cylindrical bodies located periodically in a two half – spaces medium. By considering that the number of irregularities in a period is finite and by using the periodic Green's function of two half spaces medium with planar interface, the problem is reduced to the solution of a Fredholm integral equation of second kind. The periodic Green's function of two half spaces medium with planar interface is calculated via Floquet mode expansion. Here, the resulting Fredholm integral equation is solved via an application of Method of Moments (MoM) by reducing it to a linear system of equations. The method yields quite accurate results even for surfaces having large variations. This method can also be used to solve the scattering problems of rough surfaces of infinite extend and having a localized roughness. In such a case, it is assumed that the local rough surface is periodically repeated in one direction which allows one to formulate the problem as a scattering from a periodic rough surface. In order to have an accurate model, the period should be chosen large enough as compared to the length of the rough part. Numerical simulations show that the method yields effective and accurate results for surfaces of arbitrary variation.

## ENGEBELİ PERİYODİK YÜZEYLERDEN SAÇILMA PROBLEMLERİNİN ÇÖZÜMÜ İÇİN PERİYODİK GÖMÜLÜ CİSİM YAKLAŞIMI

### ÖZET

Bu tez çalışmasında, elektromanyetik dalgaların periyodik engebeli dielektrik yüzeylerden saçılmasına yönelik yeni bir yöntem ele alınmıştır. Ele alınan yöntem, Periyodik Gömülü Cisim Yaklaşımı, sonsuz uzunluktaki engebeli yüzeylerden saçılma problemini çözen Gömülü Cisim Yaklaşımı'nın periyodik yüzeylere uygulanmasıyla elde edilmiştir. Periyodik Gömülü Cisim Yaklaşımı'ndaki temel prensip, düzlemsel arayüz ile ayrılan periyodik iki boyutlu uzayda engebeli yüzeylerin engebelerinin gömülü cisim olarak varsayılmasıdır. Bu yaklaşım, problemin iki boyutlu uzayda yer alan silindirik cisimlerden saçılması şeklinde formüle edilmesini sağlar. Bir periyottaki düzensizliklerin sonlu kabul edilmesi ve iki boyutlu uzayın periyodik Green's fonksiyonunun kullanılması ile problem ikinci tür bir Fredholm integral eşitliği probleminin çözümüne indirgenir. İki boyutlu uzayın periyodik Green's fonksiyonu efektif yöntemler kullanılarak sayısal hesaplamaları yapılan Floquet mod açılımıyla hesaplanır. Burada, Fredholm integral eşitliği Method of Moments (MoM)'in lineer sistem eşitliklerine indirgenmesiyle elde edilir. Tezde ele alınan Periyodik Gömülü Cisim Yaklaşımı, büyük salınımlar yapan yüzeyler için dahi çok iyi sonuçlar vermektedir. PBOA, aynı zamanda sonsuz uzunlukta olup bölgesel engebeye sahip yüzeylerden saçılma problemlerinin çözümünde de kullanılabilir. Bu durumda, bölgesel engebeli yüzeyin bir yönde periyodik olarak tekrarlandığı varsayılarak problemin periyodik bir yüzeyden saçılma problemi şeklinde formüle edilmesi sağlanır. Bu tarz problemleri çözerken doğru sonuçlar elde etmek için periyodun engebeli parçaya oranla yeterince büyük olması gerekmektedir. Sayısal simülasyonlar, yeni olan bu yöntemin rasgele dağılıma sahip yüzeyler için efektif ve doğru sonuçlar verdiğini göstermektedir.

## 1. INTRODUCTION

Periodic structures appear in many applications such as antenna design, microwave systems, metamaterials, integrated optics etc. and the analysis of electromagnetic wave propagation in periodic structures constitutes an important and interesting class of problems in electromagnetic theory due to its applications [1-4]. Among them scattering of electromagnetic waves from periodic surfaces have been of considerable interest to scientists and engineers for many years since they are of practical importance in designing reflection and transmission gratings often used as filters, broadband absorbers, and polarizers, and in the study of reflection by periodic surfaces such as the sea on radar systems [5].

The analysis of wave propagation in periodic structures was first investigated as early as 1887 by Lord Rayleigh. At the end of the nineteenth century and early twentieth century many scientists (Vaschy, Pupin, Campbell) used periodic networks to develop electric filters. In 1928, the problem of an atomic grating subject to a periodic sinusoidal potential and the behavior of particles in force fields that are characterized by sinusoidal and rectangular periodic variations was analyzed by Strutt and Van der Pol. In the same year, the solutions of the use of partial differential equations with periodic equations as a result of Floquet composed the base of the theory of electrons in crystals, i.e., of the theory of solids and energy bands. The periodic structures were also of considerable interest in the field of optical multilayers that have applications such as filters, antireflection films, beam splitters, and polarizers. In the 1950's, the main emphasis in the fields of periodic structures was due to slow wave structures and antennas. In the 1960's, the solution of the electromagnetic wave equation in sinusoidally periodic and laminar media, wave propagation in time and space-time periodic media, and localized source radiation had generated a new interest in the field of periodic structures. In the early 1970's, due to technological achievements the idea that the new materials having the properties such as nonlinear, piezoelectric, anisotropic, magnetoelastic etc. could be used in the forms of bulk, thin film, fibers with very good periodicities to help

electromagnetic, acoustic and electron waves stimulated the studies of the waves in periodic structures. In addition, the properties of periodic structures were of important interest in the fields of structural engineering, classical acoustic, liquid crystals, and insect vision. [6]. In the following decades, enormous efforts have been devoted to the investigation of the periodic structures in such fields and several analytical and numerical techniques have been developed.

Finally, being faced in nature in the form of crystals, being generated by a standing wave, an acoustic wave in a fluid or solid, or an electromagnetic wave in a nonlinear or active medium, being produced by repeating a unit cell the periodic structures attracted the scientists' attention to study their characteristics. However, what made the periodic structures so unique and important is their eigenmodes which are composed of an infinite number of space-harmonics with phase-velocities from zero to infinity and their support to propagating waves only in well-specified propagation bands. [6]

Periodic surfaces in interest may be a perfectly conducting one [5, 7-10] or an interface separating two dielectric media [11-14]. The most common methodology for solving scattering problems related to periodic surfaces is based on the Rayleigh Hypothesis which is only valid for surfaces having a sinusoidal variation [14, 15] and small slopes compared to wavelengths. In such a case, the scattered field is assumed to be represented in terms of discrete spectrum of outgoing plane waves [15]. The boundary element method [3-4] and method of moments (MoM) [5] are among the most frequently used approaches in the solution of scattering problems related to periodic surfaces. In [4], the problem is solved by reducing it to coupled type surface integral equations which are solved by boundary element method. The interesting part of this work is the application of the solution procedure to the analysis of anechoic chamber absorbers.

Within this framework, this paper aims to give a new and effective method for the solution of scattering problems related to periodic dielectric rough surfaces. The method is the extension of Buried Object Approach (BOA) given in [16, 17, 18] to the present problem. For the sake of simplicity, periodic surfaces in one direction are considered. The basic idea in the BOA is to assume the fluctuations of the rough surface from the flat one as buried objects in a periodic two half - spaces medium with planar interface.

Such an approach allows formulating the problem as a scattering of electromagnetic waves from cylindrical bodies located periodically in a two half – spaces medium. By considering that the number of irregularities in a period is finite and by using the periodic Green's function of two half spaces medium with planar interface, the problem is reduced to the solution of a Fredholm integral equation of second kind. The periodic Green's function of two half spaces medium with planar interface is calculated via Floquet mode expansion [15] and we utilize the efficient calculation methodologies in its numerical evaluation [19]. The resulting Fredholm integral equation is solved via an application of Method of Moments (MoM) by reducing it to a linear system of equations. The method yields quite accurate results even for surfaces having large variations. The length of the period as well as the number of irregularities of the roughness affects the computational cost of the method.

The theory developed here can also be used for solving scattering problems related to surfaces of infinite extent and having a local roughness. In such a case, it is assumed that the local rough surface is periodically repeated in one direction which allows one to formulate the problem as a scattering from a periodic rough surface.

In order to have an accurate model, the period should be chosen large enough as compared to the length of the rough part. Note that in the BOA solution one has to use the Green's function of a two half-space medium which involves the calculation of the Sommerfeld type integrals. This usually increases the computational cost. On the other hand in the periodic model we use only Green's function of the periodic medium which can only be calculated in terms of Floquet modes. Numerical solutions show that the model is quite accurate and computationally less expensive.

In section 2, a general formulation and the Floquet Theorem are given while the application of the BOA to the periodic surfaces is described in section 3. Section 4 is devoted to the solution of Fredholm integral equation of second kind by an application of MoM. Numerical results are presented in section 5. Throughout this work, a time factor  $e^{-i\omega t}$  is assumed and omitted.

## 2. FORMULATION OF THE PROBLEM

### 2.1 Geometry of the Problem

Consider the two-dimensional scattering problem related to the periodic structure given in Figure 2.1, where the upper and lower dielectric half spaces are separated by the periodic interface  $\Gamma_0$  having a period  $L$ . In each period the interface is either represented by the function  $x_2 = f(x_1 + pL)$ ,  $x_1 \in (0, L)$ ,  $p = 0, \pm 1, \pm 2, \dots$ , where  $f(x_1)$  a single valued function [20] is or it can be a random one with rms height  $h$ , correlation length  $\ell$ . The half-spaces above and below  $\Gamma_0$  are assumed to be filled with simple non-magnetic materials having dielectric permittivities and conductivities  $\epsilon_1, \sigma_1 = 0$  and  $\epsilon_2, \sigma_2$  respectively.

The scattering problem considered here is to determine the effect of  $\Gamma_0$  on the propagation of electromagnetic waves excited in the upper half-space  $x_2 > f(x_1)$ , more precisely to obtain the scattered field from the surface  $\Gamma_0$  in each period. To this aim, the half-space  $x_2 < f(x_1)$  is illuminated by a time-harmonic plane wave whose electric field vector is always parallel to the  $Ox_3$  axis, namely,

$$\vec{E}_i = (0, 0, u_i(x_1, x_2)) \quad (2.1)$$

which can be written as [16]

$$u_i(x_1, x_2) = A_0 e^{-i\beta x_1} e^{\gamma_1 x_2} \quad (2.2)$$

where  $\beta = k_1 \cos \phi_0$  with  $\phi_0 \in (0, \pi)$  being the incidence angle while  $k_1$  stands for the wave number of the upper half-space which is defined by  $k_1 = \omega \sqrt{\epsilon_1 \mu_0}$ . The square root function  $\gamma_1(\beta) = \sqrt{\beta^2 - k_1^2}$  appearing in (2) is defined as  $\gamma_1(0) = -ik_1$  in the properly cut complex  $\beta$ - plane. Since the problem is homogenous in the  $Ox_3$  direction, the problem

is reduced to a 2D scalar one in terms of the total field function  $u(x)$ , where the total electric field vector is defined by  $\vec{E} = (0, 0, u(x))$  solution.

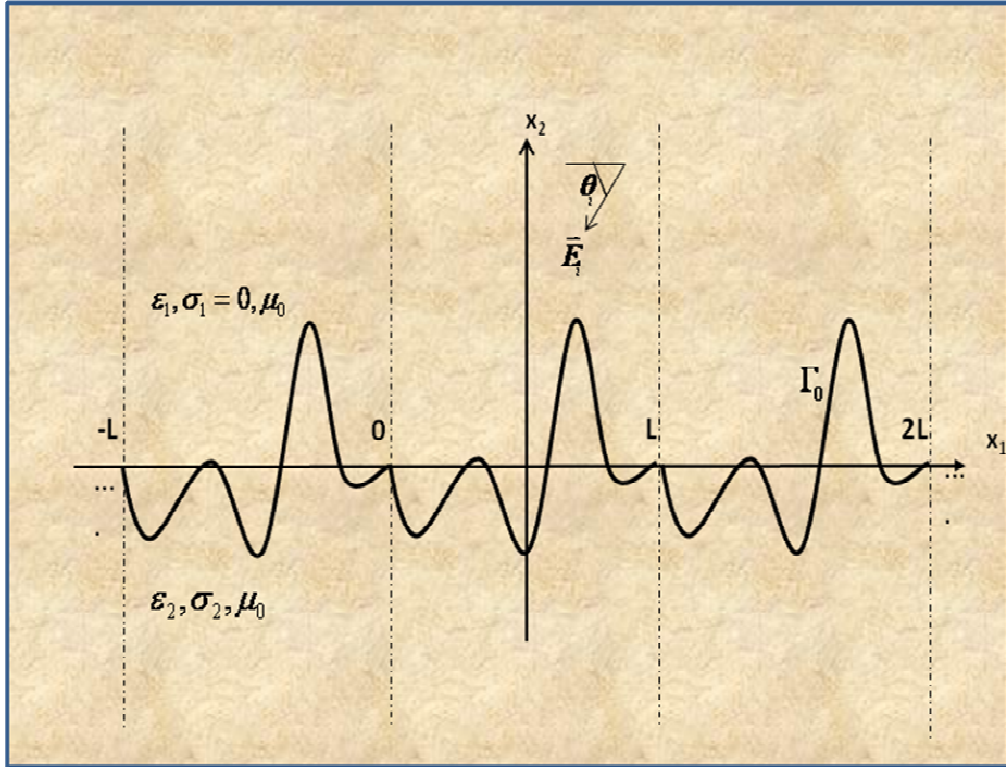


**Figure 2.1:** Geometry of the problem

In order to adapt the formulation to this type of problem, a Floquet expansion is applied. In the following, the Floquet theorem which is the starting point of solving the problems of periodic structures will be explained.

## 2.2 The Floquet Theorem

Consider a wave propagating in periodic structures, as shown in Figure 2.2. The fields at a point  $z$  in an infinite periodic structure differ from the fields one period  $L$  away by a complex constant since there should be no difference between the fields at  $z$  and at  $z + L$  except for the constant attenuation and phase shift. Let a function  $u(z)$  represent a wave. Then a wave  $u(z)$  at a point  $z$  and a wave  $u(z + L)$  at  $z + L$  are related in the same manner as a wave  $u(z + L)$  at  $z + L$  and a wave  $u(z + 2L)$  at  $z + 2L$ .



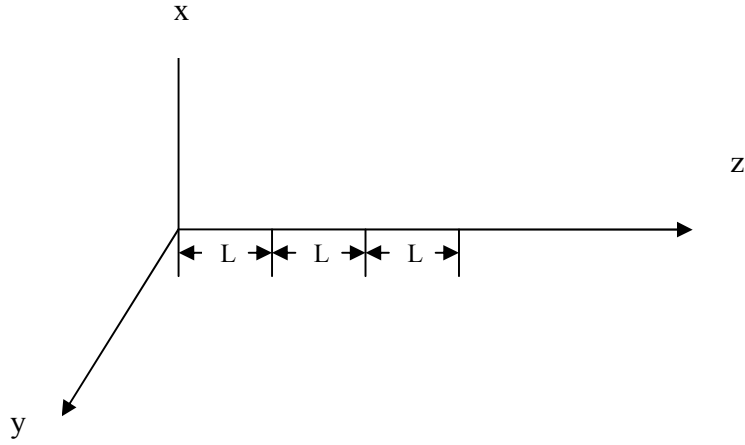


**Figure 2.2:** Periodic structures

So mathematically, it can be written as

$$\frac{u(z+L)}{u(z)} = \frac{u(z+2L)}{u(z+L)} = \frac{u(z+mL)}{u[z+(m-1)L]} = C = \text{constant} \quad (2.3)$$

$$u(z+mL) = C^m u(z) \quad (2.4)$$

The constant  $C$  can be written as

$$C = e^{-j\beta L} \quad (2.5)$$

where  $\beta$  is the complex propagation constant.

Let us consider a function

$$R(z) = e^{j\beta L} u(z) \quad (2.6)$$

Then  $R(z+L) = e^{j\beta(z+L)} u(z+L) = R(z)$ . Therefore,  $R(z)$  is a periodic function of  $z$  with the period  $L$ , and thus can be represented in a Fourier series.

$$R(z) = \sum_{-\infty}^{\infty} A_n e^{-j(2n\pi/L)z} \quad (2.7)$$

Using (2.5) the general expression for a wave in a periodic structure with the period  $L$  is obtained as

$$u(z) = \sum A_n e^{-j\beta_n z} \quad (2.8)$$

where

$$\beta_n = \beta + \frac{2n\pi}{L} \quad (2.9)$$

This is a representation of a wave in periodic structures in a form of an infinite series resembling harmonic representation ( $e^{-j\omega_n t}$ ) in time. The  $n$ th term in (2.8) is called  $n$ th space harmonic. Equation (2.7) is the mathematical representation of Floquet theorem for outgoing waves, which states that the wave in periodic structures consists of an infinite number of space harmonics.

According to the Floquet theorem the scattered field distribution of a periodic structure as in Figure 2.1 remains unchanged under a translation of the observation point in the  $x_1$ -direction through a period  $L$  while its amplitude is multiplied by a complex constant  $e^{j\beta L}$  which corresponds to the variation of the incident field with  $x_1$ . Invoking the Floquet theorem, the problem can be readily reduced to a consideration of the fields over a single period of  $L$ . Then the total field  $u$  in a single period  $x_1 \in (0, L)$  satisfies the reduced wave equation

$$\Delta u + k^2(x)u = 0, \quad x_1 \in (0, L) \quad (2.10)$$

with

$$k^2(x) = \begin{cases} k_1^2, & x_2 > f(x_1) \\ k_2^2, & x_2 < f(x_1) \end{cases} \quad (2.11)$$

under the boundary conditions

$$u \text{ and } \frac{\partial u}{\partial n} \text{ are continuous on } \Gamma_0. \quad (2.12)$$

In (2.11)  $k_2$  is the wave number of the half-space  $x_2 < (x_1)$  which is defined as the square root of  $k_2^2 = \omega^2 \varepsilon_2 \mu_0 + i\omega \sigma_2 \mu_0$ .

Note that the scattered field defined as  $u_s(x) = u(x) - u_0(x)$  satisfies the classical quasi-periodic radiation condition expressed by the Floquet series of the scattered wave [24, 25]. Here  $u_0(x)$  is the total electric field in a single period in the case of the interface is a flat one. This field can be obtained very easily and one has

$$u_0(x) = \begin{cases} u_i(x) + R_{12}(\beta) e^{-i\beta x_1 - \gamma_1 x_2}, & x_2 > 0 \\ T_{12}(\beta) e^{-i\beta x_1 + \gamma_2 x_2}, & x_2 < 0 \end{cases} \quad (2.13)$$

where  $R_{12}$  and  $T_{12}$  are the reflection and transmission coefficients of the plane  $x_2 = 0$ , respectively and given by

$$R_{12}(\beta) = \frac{\gamma_1(\beta) - \gamma_2(\beta)}{\gamma_1(\beta) + \gamma_2(\beta)} \quad (2.14)$$

$$T_{12}(\beta) = \frac{2\gamma_1(\beta)}{\gamma_1(\beta) + \gamma_2(\beta)} \quad (2.15)$$

with

$\gamma_2(\beta) = \sqrt{\beta^2 - k_2^2}$ ,  $\gamma_2(0) = -ik_2$ . It is well known that this problem can be treated very easily when the roughness of the interface is in the limitations of the Rayleigh Hypothesis by using the Floquet Theorem where the field is represented in terms of Floquet modes inside each period [17]. Note that the solution based on Rayleigh Hypothesis is valid for periodic rough surfaces satisfying the condition  $2\pi h / L < 0.448$  where  $h$  is the maximum peak point of the the surface [14]. In the following, we will

give a method which is valid beyond the Rayleigh limits and for surfaces of arbitrary variation.

### **3. PERIODIC BURIED OBJECT MODELLING**

In this section, the application of a method called buried object approach (BOA) to periodic surfaces will be described. Before giving the details of periodic buried object approach (PBOA) a brief survey of BOA modelling will be given.

#### **3.1 Buried Object Approach**

BOA, an efficient method for the scattering of electromagnetic waves from dielectric rough surfaces of infinite extent was introduced in [18-20]. The method in [19] is for the scattering of electromagnetic waves from a locally rough interface between two dielectric half – spaces. It is based on the assumption that the perturbations of the rough surface from the planar interface are objects buried in a media of two half spaces with a planar boundary. This allows one to reduce the problem to the scattering of electromagnetic waves by cylindrical bodies of arbitrary cross section. Then through the Green's function of the background medium one obtains a Fredholm integral equation of the second kind, which is solved via an application of the MoM. The present formulation permits one to get the near and far field expressions of the scattered wave. This method gives very accurate results for the surfaces which are locally rough, rapidly varying and having large rms height. One of the main difficulties in the application of this method is that it requires computing the Green's function of the two half spaces medium, which usually involves the computation of Sommerfeld integrals causing the method to be computationally expensive. On the other hand, the Green's function of a periodic two-half spaces media with planar interface can be calculated in terms of Floquet mode expansion [21] and its numerical evaluation is not costly. By taking this property into account, one can consider to extend the BOA method to the scattering by periodic rough interfaces, which from now on will be called as PBOA.

### 3.2 Periodic Buried Object Approach

In PBOA modeling, the whole space is separated into two parts by the plane  $x_2 = 0$ . In such a case, one has domains bounded by the rough surface  $\Gamma_0$  and the plane  $x_2 = 0$  which are located periodically in a two half-space media with planar interface (see Figure 3.1). Then the problem can be considered as scattering of electromagnetic waves from periodically located cylindrical bodies in a layered media. In the following, it will be assumed that the number of the cylindrical bodies in a period is  $N$ , having cross sections  $B_1, B_2, \dots, B_N$  with the  $Ox_1x_2$  plane.

By considering the periodic Green's function  $G_p(x; y)$  of the two-half spaces media, the problem can be reduced to the solution of the following Fredholm integral equation of second kind for the total field  $u$  within the period  $x_1 \in (0, L)$ .

$$u(x) = u_0(x) + \sum_{n=1}^N \int_{B_n} G_p(x; y) \nu(y) u(y) dy \quad (3.1)$$

where

$$\nu_n(x) = \begin{cases} k_1^2 \left( \frac{\varepsilon_2^i}{\varepsilon_1} - 1 \right), & x \in B_n, \quad x_2 > 0 \\ k_2^2 \left( \frac{\varepsilon_1^i}{\varepsilon_2} - 1 \right), & x \in B_n, \quad x_2 < 0 \end{cases} \quad (3.2)$$

in which  $\varepsilon_2^i = \varepsilon_2 + i\sigma_2 / \omega$  stands for the complex dielectric permittivity of the lower half-space. Note that by taking the quasi-periodicity of the field into account, the total field in the  $p$ 'th period can be written as  $e^{i\beta_p L} u(x)$ , where  $\beta_p = k_1 \cos \theta + \frac{2\pi p}{L}$ .

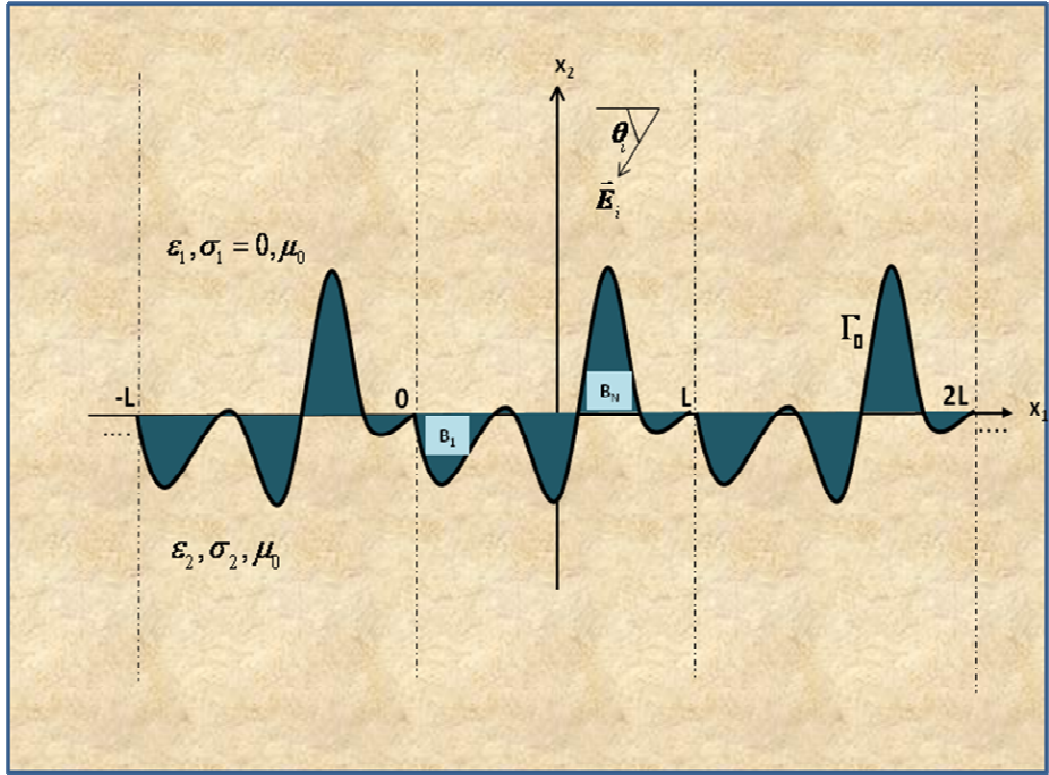


**Figure 3.1:** Buried object modeling of the rough surface

In Section 4, the method based on MoM to solve  $u(x)$  from (3.1) will be given. Before going further, it will be convenient to give an explicit expression of the Green's function  $G_p(x; y)$ .

By definition, the  $G_p(x; y)$  satisfies the reduced wave equation

$$\Delta G_p(x; y) + k^2(x_2)G_p(x; y) = -J_a(x, y) \quad (3.3)$$

with

$$k^2(x) = \begin{cases} k_1^2, & x_2 > 0 \\ k_2^2, & x_2 < 0 \end{cases} \quad (3.4)$$

and

$$J_a(x, y) = \sum_{p=-\infty}^{\infty} \delta(x_1 - y_1 - pL)\delta(x_2 - y_2). \quad (3.5)$$

In this equation  $y \in \square^2$  is an arbitrary point and  $\delta$  is the Dirac's delta distribution. Following the same procedure given in [21] one can show that the periodic Green's function for the present problem is given by

$$G_p(x; y) = \begin{cases} \sum_{p=-\infty}^{\infty} \left[ \frac{i}{4} H_0^1(k_1 \sqrt{(x_1 - y_1 - pL)^2 + (x_2 - y_2)^2}) \right. \\ \left. + \frac{1}{L} \frac{1}{2\gamma_1(\beta_p)} e^{i\beta_p(x_1 - y_1)} R_{12}(\beta_p) e^{-\gamma_1(\beta_p)(x_2 + y_2)} \right], & x_2 > 0, y_2 > 0 \\ \frac{1}{L} \sum_{p=-\infty}^{\infty} \frac{1}{2\gamma_1(\beta_p)} T_{12}(\beta_p) e^{i\beta_p(x_1 - y_1)} e^{-\gamma_1(\beta_p)y_2 + \gamma_2(\beta_p)x_2}, & x_2 < 0, y_2 > 0 \\ \frac{1}{L} \sum_{p=-\infty}^{\infty} \frac{1}{2\gamma_1(\beta_p)} T_{21}(\beta_p) e^{i\beta_p(x_1 - y_1)} e^{-\gamma_1(\beta_p)x_2 + \gamma_2(\beta_p)y_2}, & x_2 > 0, y_2 < 0 \\ \sum_{p=-\infty}^{\infty} \left[ \frac{i}{4} H_0^1(k_2 \sqrt{(x_1 - y_1 - pL)^2 + (x_2 - y_2)^2}) \right. \\ \left. + \frac{1}{L} \frac{1}{2\gamma_2(\beta_p)} e^{i\beta_p(x_1 - y_1)} R_{12}(\beta_p) e^{-\gamma_2(\beta_p)(x_2 + y_2)} \right], & x_2 > 0, y_2 < 0 \end{cases} \quad (3.6)$$

where

$$T_{21}(\beta) = \frac{2\gamma_2(\beta)}{\gamma_1(\beta) + \gamma_2(\beta)} \quad (3.7)$$

Note that the convergence of the Hankel function series appearing in (14) is quite poor for the values of  $x$  close to  $y$  while the exponential series converges rapidly after  $p$  exceeds values satisfying  $\text{Re}(\gamma_i(\beta_p)) > 0$ ,  $i = 1, 2$  due to the exponential decay. Thus the exponential series can be truncated at the smallest  $P$  with  $\text{Re}(\gamma_i(\beta_p)) > 0$ ,  $i = 1, 2$ . The value of the truncation number  $P$  increases with the increasing values of  $k_i$ ,  $i = 1, 2$  and period  $L$ . As to the Hankel series, one needs to use efficient techniques to accelerate the convergence such as the ones given in [20, 21]. On the other hand, by considering the asymptotic behavior of  $H_0^1$  for large arguments, one can conclude that the truncation



number  $P$  for the Hankel series is inversely proportional to the wave-number  $k_i$ ,  $i = 1, 2$  and period  $L$ .

#### 4. A METHOD OF MOMENT SOLUTION

In the sequel, to solve  $u(x)$  from (2.16) [26] a method which is an application of MoM will be described. To this aim, the equation (2.16) is written in an abbreviated form as

$$(I - K)u(x) = u_0(x), \quad x \in \square^2 \quad (4.1)$$

where  $K$  is the linear operator defined by

$$Ku(x) = \sum_{n=1}^N \int_{B_n} G_p(x; y) v_n(y) u(y) dy \quad (4.2)$$

Consider now the integral on the  $n$ 'th region  $B_n$  appearing in (3.2). Due to the definition of  $v_n$ , it is a constant in  $B_n$  and it can be taken out of the integration. In order to calculate the remaining integral,  $B_n$  is divided into  $M_n$  small cells which allows one to write

$$\int_{B_n} G_p(x; y) u(y) dy = \sum_{m=1}^{M_n} \int_{S_{nm}} G_p(x; y) u(y) dy \quad (4.3)$$

where  $S_{nm}$  denotes  $m$ 'th cell of the region  $B_n$ . If  $S_{nm}$  is small enough one can make the approximation  $u(y) \approx u(y^{nm})$  for the total field inside the related cell, where  $y^{nm} = (y_1^{nm}, y_2^{nm})$  stands for the center point of the cell  $S_{nm}$ . Then one has

$$\int_{B_n} G_p(x; y) u(y) dy \approx \sum_{m=1}^{M_n} u(y^{nm}) C^{nm}(x) \quad (4.4)$$

Here we put

$$C^{nm}(x) = \int_{S_{nm}} G_p(x; y) dy \quad (4.5)$$

When the geometry of  $S_{nm}$  is given the coefficients  $C_{nm}(x)$  can be calculated through (3.6) and (4.5). For a rectangular cell with side lengths  $2\Delta y_1 * 2\Delta y_2$ ,  $C_{nm}(x)$  will be

$$C^{nm}(x) = \begin{cases} C_0^{nm}(x) + C_1^{nm}(x), & x_2 > 0, y_2^{nm} > 0 \\ C_2^{nm}(x), & x_2 < 0, y_2^{nm} > 0 \\ C_3^{nm}(x), & x_2 > 0, y_2^{nm} < 0 \\ C_4^{nm}(x) + C_5^{nm}(x), & x_2 < 0, y_2^{nm} < 0 \end{cases} \quad (4.6)$$

where

$$C_0^{nm}(x) = \begin{cases} \frac{i}{2k_1^2} [\pi k_1 a H_1^1(k_1 a) + 2i] - \frac{\pi a}{k_1} \sum_{p=1}^{\infty} J_1(k_1 a) Y_0(pL), & x = y^{nm} \\ \sum_{p=-\infty}^{\infty} \frac{i\pi a}{2k_1} J_1(k_1 a) H_0^1(k \sqrt{(x_1 - y_1^{nm} - pL)^2 + (x_2 - y_2^{nm})^2}), & x \neq y^{nm} \end{cases} \quad (4.7)$$

$$C_1^{nm}(x) = \frac{4}{L} \sum_{p=-\infty}^{\infty} \frac{1}{2\gamma_1(\beta_p)} R_{12}(\beta_p) \frac{\sinh(\gamma_1(\beta_p)\Delta y_2)}{\gamma_1(\beta_p)} \frac{\sin(\beta_p \Delta y_1)}{\beta_p} e^{i\beta_p(x_1 - y_1^{nm})} e^{-\gamma_1(\beta_p)(x_2 + y_2^{nm})}, \quad (4.8)$$

$$C_2^{nm}(x) = \frac{4}{L} \sum_{p=-\infty}^{\infty} \frac{1}{2\gamma_1(\beta_p)} T_{12}(\beta_p) \frac{\sinh(\gamma_1(\beta_p)\Delta y_2)}{\gamma_1(\beta_p)} \frac{\sin(\beta_p \Delta y_1)}{\beta_p} e^{i\beta_p(x_1 - y_1^{nm})} e^{-\gamma_1(\beta_p)y_2^{nm} + \gamma_2(\beta_p)x_2}, \quad (4.9)$$

$$C_3^{nm}(x) = \frac{4}{L} \sum_{p=-\infty}^{\infty} \frac{1}{2\gamma_1(\beta_p)} T_{21}(\beta_p) \frac{\sinh(\gamma_2(\beta_p)\Delta y_2)}{\gamma_2(\beta_p)} \frac{\sin(\beta_p \Delta y_1)}{\beta_p} e^{i\beta_p(x_1 - y_1^{nm})} e^{-\gamma_1(\beta_p)x_2 + \gamma_2(\beta_p)y_2^{nm}}, \quad (4.10)$$

$$C_4^{nm}(x) = \frac{4}{L} \sum_{p=-\infty}^{\infty} \frac{-1}{2\gamma_1(\beta_p)} R_{12}(\beta_p) \frac{\sinh(\gamma_2(\beta_p)\Delta y_2)}{\gamma_2(\beta_p)} \frac{\sin(\beta_p\Delta y_1)}{\beta_p} e^{i\beta_p(x_1 - y_1^{nm})} e^{\gamma_2(\beta_p)(x_2 + y_2^{nm})}, \quad (4.11)$$

$$C_5^{nm}(x) = \begin{cases} \frac{i}{2k_2^2} [\pi k_2 a H_1^1(k_2 a) + 2i] - \frac{\pi a}{k_2} \sum_{p=1}^{\infty} J_1(k_2 a) Y_0(pL), & x = y^{nm} \\ \sum_{p=-\infty}^{\infty} \frac{i\pi a}{2k_2} J_1(k_2 a) H_0^1(k_2 \sqrt{(x_1 - y_1^{nm} - pL)^2 + (x_2 - y_2^{nm})^2}), & x \neq y^{nm} \end{cases} \quad (4.12)$$

In (4.7) and (4.12) "a" denotes the radius of the circular cell whose area is equivalent to the rectangular cell  $2\Delta y_1 * 2\Delta y_2$  [27].

Substituting (4.4) into (4.3) and writing (3.1) for  $x = y^{pq}$ ,  $p = 1, 2, \dots, N$ ,  $q = 1, 2, \dots, M_p$  one gets a linear system of equations for the field values of  $u(y^{pq})$ . Note that in such a case the operator  $K$  is reduced to a square matrix with dimensions  $(M_1 + M_2 + \dots + M_N) * (M_1 + M_2 + \dots + M_N)$  and the number of unknowns in the linear system is  $(M_1 + M_2 + \dots + M_N)$ .

Since the field  $u(y)$  is now known at inner points of each cell  $S_{nm}$ , one can calculate  $u(x)$  for any  $x \in \square^2$ ,  $x_1 \in (0, L)$  through the relation

$$u(x) \square u_0(x) + \sum_{n=1}^N \sum_{m=1}^{M_n} v_n(y^{nm}) u(y^{nm}) C^{nm}(x). \quad (4.13)$$

## 5. NUMERICAL IMPLEMENTATION

In this section, the accuracy and the effectiveness of the algorithm given in the previous section will be tested with some illustrative examples. In all examples, the upper half-space is assumed to be free space.

### 5.1 Sinusoidally Periodic Surface

Consider a periodic surface , as in Figure 5.1, having a sinusoidal variation of the form

$$f(x_1) = -0.02\lambda \cos\left(\frac{2\pi x_1}{\lambda}\right), \quad x_1 \in (0, L) \quad (5.1)$$

where  $\lambda$  is the free-space wavelength. Note that the maximum slope of the surface is  $\frac{\partial f}{\partial x} = 0.1256$  which is smaller than 0.448. Thus, the Rayleigh hypothesis is satisfied and one can express the scattered field in terms of outgoing waves yielding an analytical solution [17]. The parameters of the lower half-space are  $\varepsilon_2 = 3\varepsilon_0$ ,  $\sigma_2 = 10^{-5}$  and the incidence angle is  $\phi_0 = \pi/4$ . The periodic buried object modeling yields two objects which are located in the upper and lower half-spaces in a period. The cell sizes in the application of the MoM solution are chosen  $\lambda/30 * \lambda/150$  and  $P = 3$  terms are used in the series representation of the Periodic Green's function. The computational time is 0.109 seconds for analytical method and 1.343 seconds for PBOA. In Figure 5.2, the amplitude and the phase of the scattered field on a line  $x_2 = 0.3\lambda$  in a period calculated by both the analytical and PBOA are presented. It is obvious that both results are in a very good agreement.

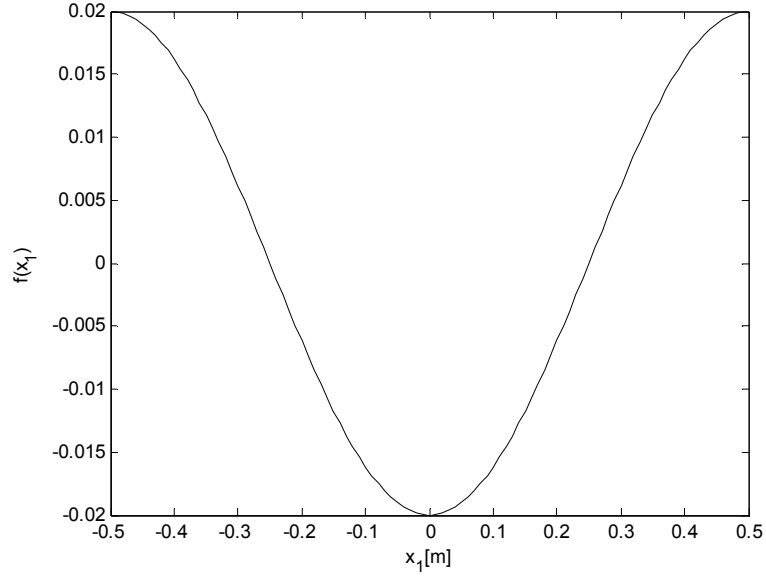


**Figure 5.1:** Sinusoidally surface profile

Similar simulations are carried out for another sinusoidal variation of the form

$$f(x_1) = -0.07\lambda \cos\left(\frac{2\pi x_1}{\lambda}\right), \quad x_1 \in (0, L) \quad (5.2)$$

The maximum slope of the surface is  $\frac{\partial f}{\partial x} = 0.439$ , which while quite close to 0.448 still satisfies the Rayleigh hypothesis. The parameters of the lower half-space are  $\varepsilon_2 = 3\varepsilon_0$ ,  $\sigma_2 = 10^{-5}$  and the incidence angle is  $\phi_0 = \pi/6$ . The cell sizes are the same as in the previous example. The amplitude and the phase of the scattered field is calculated on a line  $x_2 = 0.5\lambda$  in a period. As in Figure 5.3, both results are in a very good agreement.

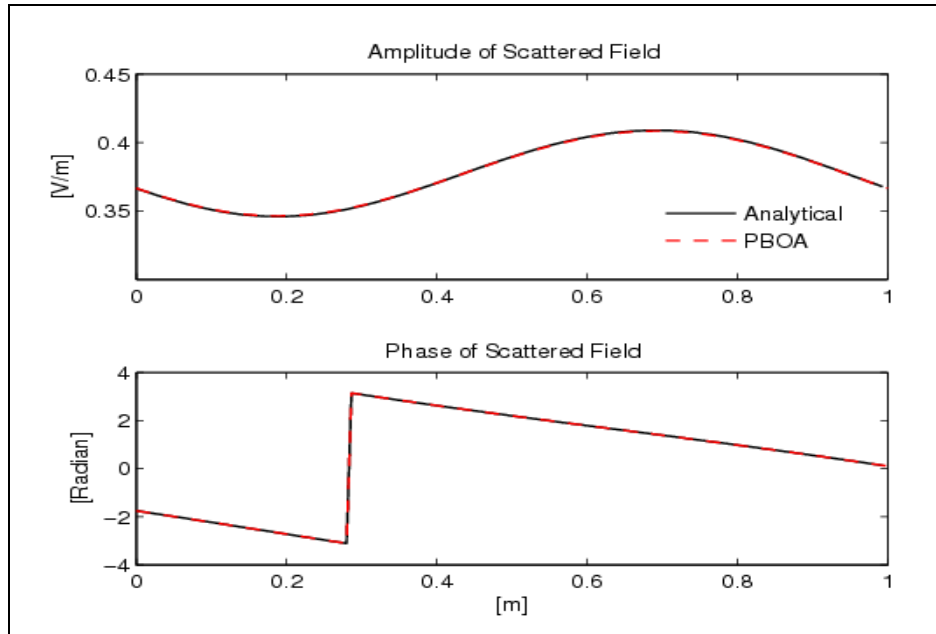


**Figure 5.2:** Comparison of the amplitude and the phase of the scattered field obtained by Analytical and PBOA methods for the surface given in (5.1)

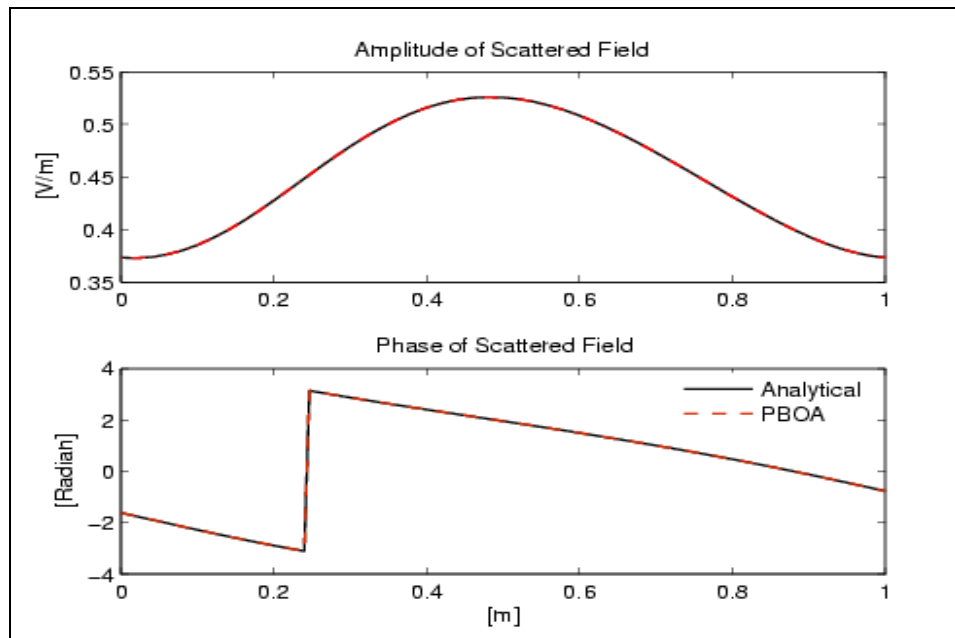


**Figure 5.3:** Comparison of the amplitude and the phase of the scattered field obtained by Analytical and PBOA methods for the surface given in (5.2)

## 5.2 Periodic Random Surface

As a second case, the results of PBOA and perturbation method [27] are compared for a random surface with rms height  $h = 0.006\lambda$ , correlation length  $\ell = 0.6\lambda$  and the period  $L = 4\lambda$ . The cell size used in the PBOA method is  $\lambda/25 * \lambda/150$  and the incidence direction is  $\phi_0 = 2\pi/3$  while the truncation number of the series for periodic Green's function is  $P = 20$ . The dielectric permittivity and conductivity of the lower medium are taken as  $\varepsilon_2 = 3.6\varepsilon_0$  and  $\sigma_2 = 10^{-5}$ . Figure 4 illustrates the variations of amplitudes and phases of the scattered fields obtained via both methods in a period. Clearly, both methods yield very close results.

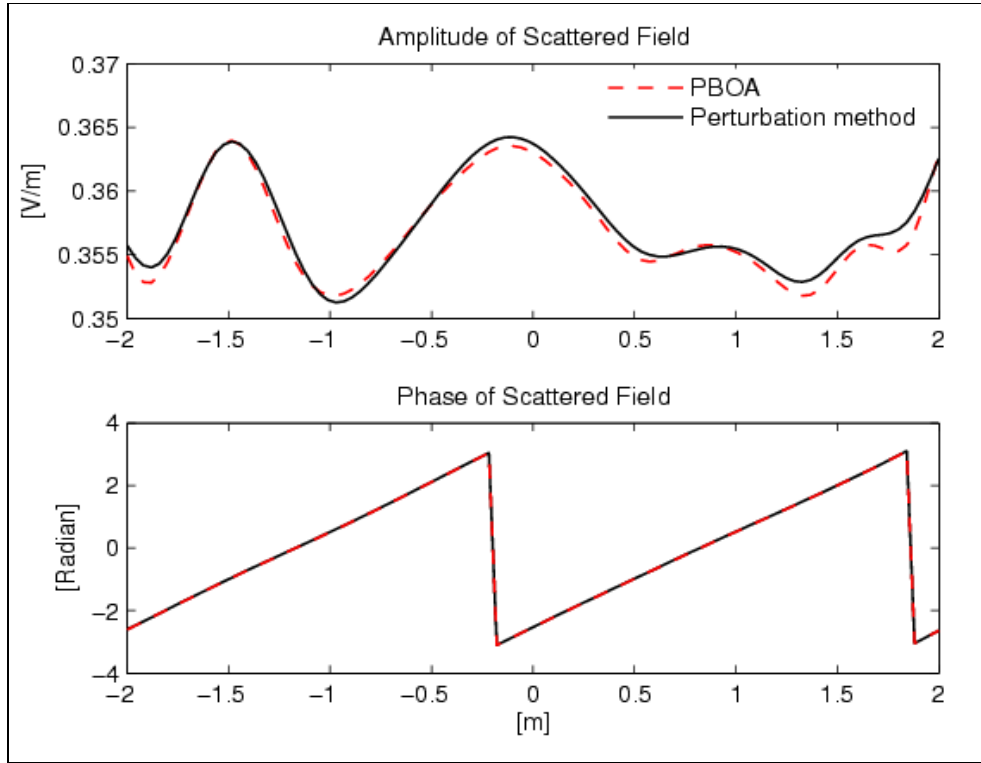


**Figure 5.4:** Comparison of the amplitude and the phase of the scattered field obtained by Perturbation and PBOA methods for the random surface of  $h = 0.006\lambda$ ,  $\ell = 0.6\lambda$  and  $L = 4\lambda$ .



### 5.3 The Effect of the Roughness on the Propagation of Incident Plane Wave

To give a physical insight about the interaction of the electromagnetic wave with the periodic rough interface, consider a random surface of rms height  $h = 0.2\lambda$ , correlation length  $\ell = 0.8\lambda$ , period  $L = 10\lambda$  with Gaussian distribution. The parameters of lower half space are chosen as in previous example and  $P = 40$ . Note that the roughness for this example is very high. Figure 5.5 shows the variation of the amplitude of the total electric field in a rectangular domain. This result allows us to see the effect of the roughness on the propagation of an incident plane wave.

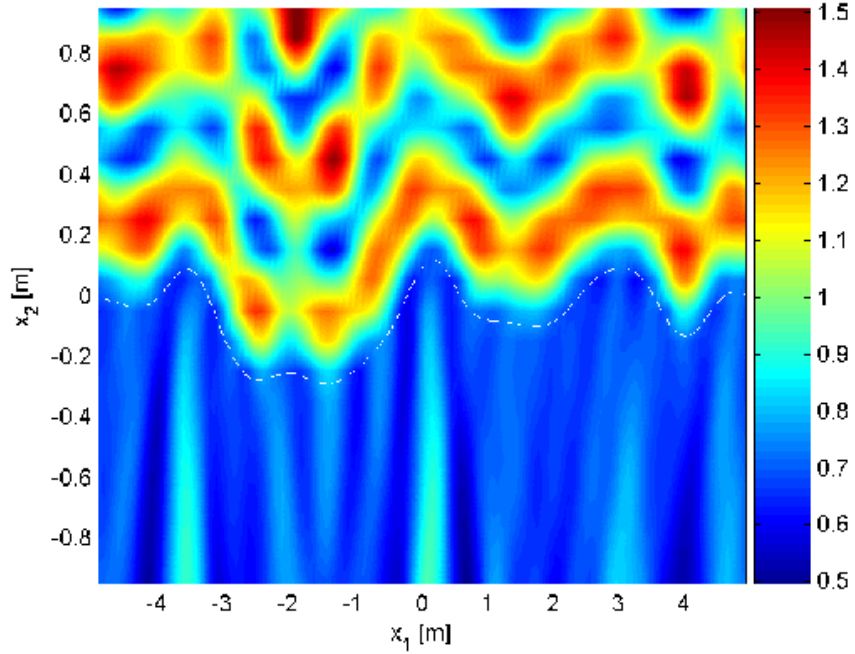


**Figure 5.5:** Variation of the total field amplitude in a rectangular region for the random periodic surface of  $h = 0.2\lambda$ ,  $\ell = 0.8\lambda$  and  $L = 10\lambda$

As a second example to see the effect of the roughness on the propagation of incident plane wave, consider a random surface of rms height  $h = 0.08\lambda$ , correlation length  $\ell = 0.8\lambda$ , period  $L = 10\lambda$ . The parameters of the lower half space are  $\varepsilon_2 = 3\varepsilon_0$ ,  $\sigma_2 = 10^{-5}$  and the incidence angle is  $\phi_0 = \pi/4$  as in previous example and  $P = 40$ . Figure 5.6 shows the variation of the amplitude of the total electric field in a rectangular domain.

In Figure 5.7 and Figure 5.8, the variations of the amplitudes of the total field for two different incidence directions  $\phi_0 = \pi/2$  and  $\phi_0 = \pi/4$  are presented for the case of a random air- mica interface with parameters  $h = 0.15\lambda$ ,  $\ell = 0.6\lambda$  and  $L = 11\lambda$ . Note that the electromagnetic parameters of mica are  $\varepsilon_2 = 5.4\varepsilon_0$ ,  $\sigma_2 = 10^{-15}$ .

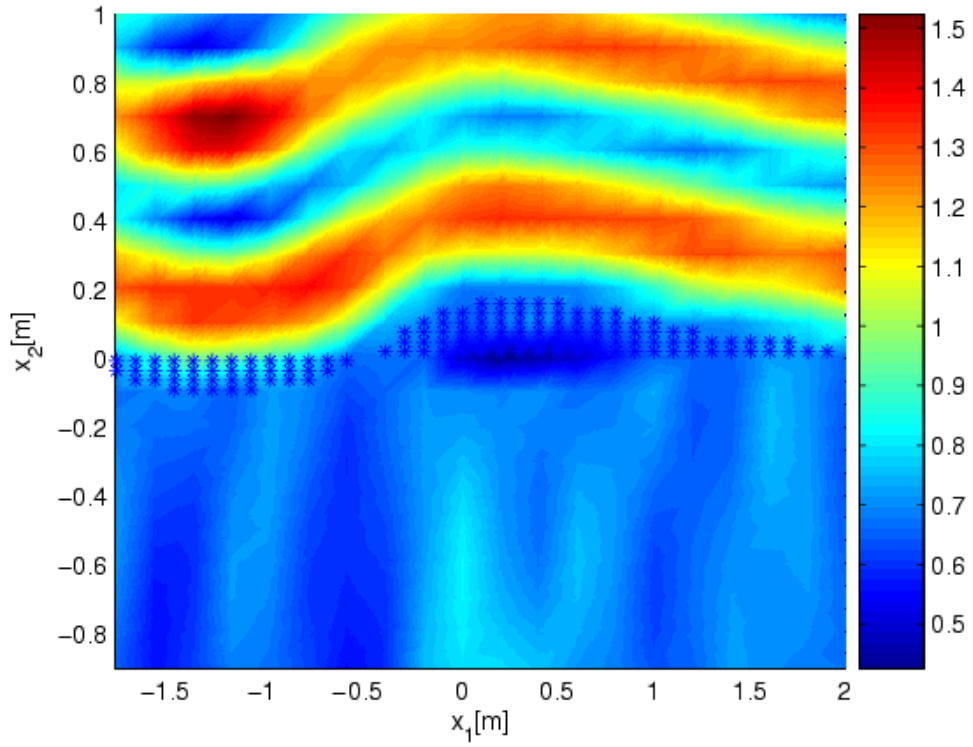


**Figure 5.6:** Variation of the total field amplitude in a rectangular region for the random periodic surface of  $h = 0.08\lambda$ ,  $\ell = 0.8\lambda$  and  $L = 10\lambda$

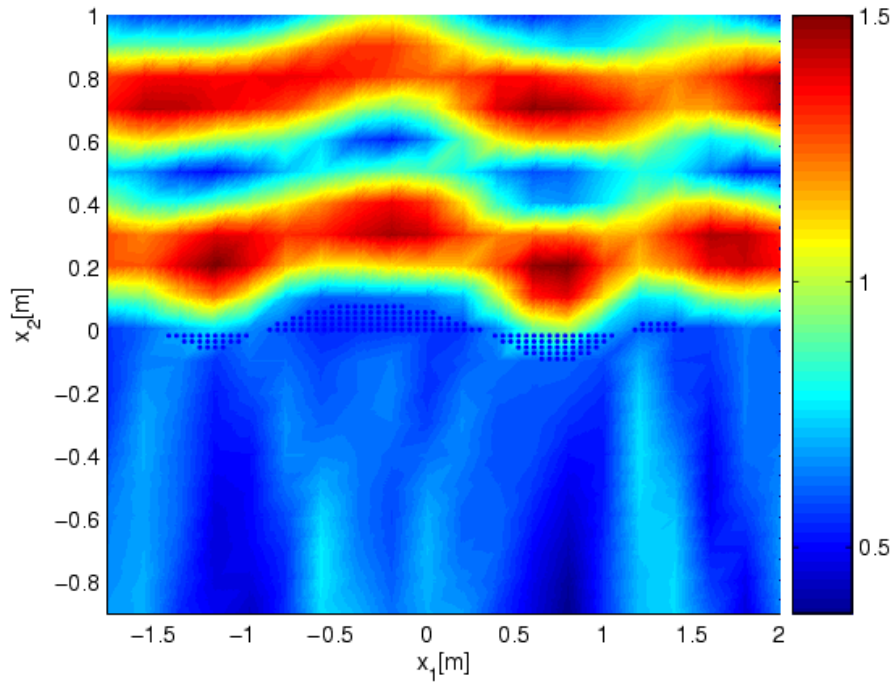


**Figure 5.7:** Variation of the total field amplitude for the random periodic air-micra interface with  $h = 0.15\lambda$ ,  $\ell = 0.6\lambda$ ,  $L = 11\lambda$  and  $\phi_0 = \pi/2$

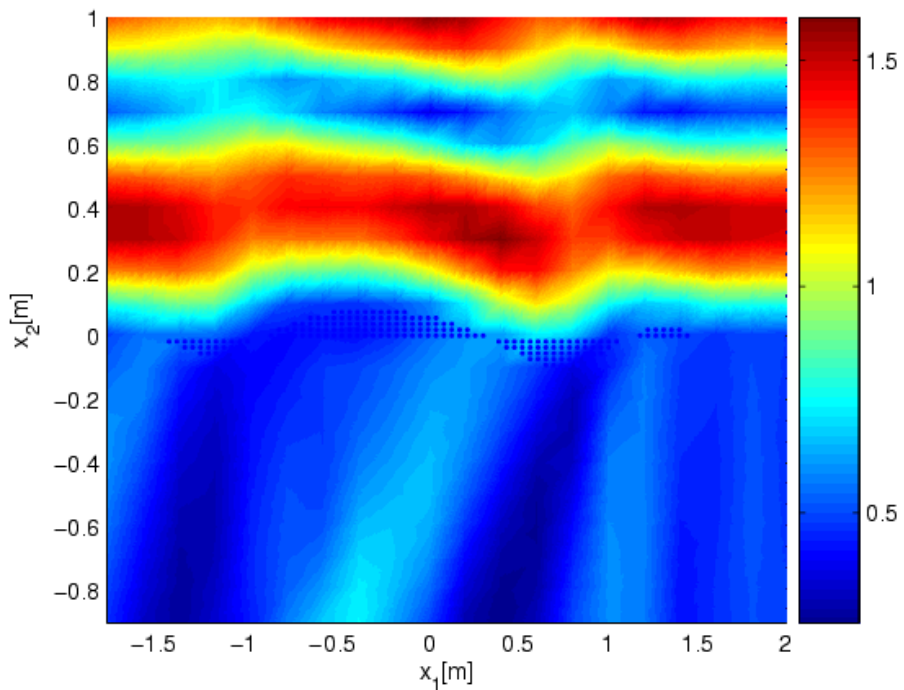


**Figure 5.8:** Variation of the total field amplitude for the random periodic air-micra interface with  $h = 0.15\lambda$ ,  $\ell = 0.6\lambda$ ,  $L = 11\lambda$  and  $\phi_0 = \pi/4$

#### 5.4 Locally Rough Surface

The PBOA presented here can also be extended to solve the scattering problems related to surfaces of infinite extent having a local roughness of length  $\ell_R$  (see Figure 5.9a). To this aim, consider a periodic rough surface of period  $L$  and assume that it has the same roughness with the infinite extent one in a period (Figure 5.9b). As long as the period  $L$  is taken large enough compared to length of rough part  $\ell_R$ , the periodic one can be used as a model to the original one for the field within a period. Note that the scattering problem of the rough surface of infinite extent can be treated by using BOA which generally involves the computation of Sommerfeld integrals in Green's function of two half-spaces medium [18-20]. This causes the method to be computationally expensive. On the other hand, in the periodic model the required Green's function can be expressed in terms of Floquet modes whose computational evaluation is not costly. Thus by using the periodic model, the scattering of electromagnetic waves from locally rough surfaces can be solved more effectively through PBOA. To see the applicability and the accuracy of this idea, some surfaces are taken into consideration, the related scattering problems by both BOA and PBOA are solved and their results are compared.

In Figure 5.10, the amplitudes and the phases of the scattered field on the line  $x_2 = 0.3\lambda$ ,  $x_1 \in (0, L)$  calculated by both PBOA and BOA are compared for a locally rough surface defined by

$$f(x_1) = \begin{cases} 0.25\lambda \sin \frac{\pi x_1}{2\lambda} \left[ 0.5 \cos \frac{2\pi x}{\lambda} - 0.25\lambda \sin \frac{2\pi x_1}{0.8\lambda} \right], & x \in (-2\lambda, 2\lambda) \\ 0, & \textit{otherwise.} \end{cases} \quad (5.3)$$

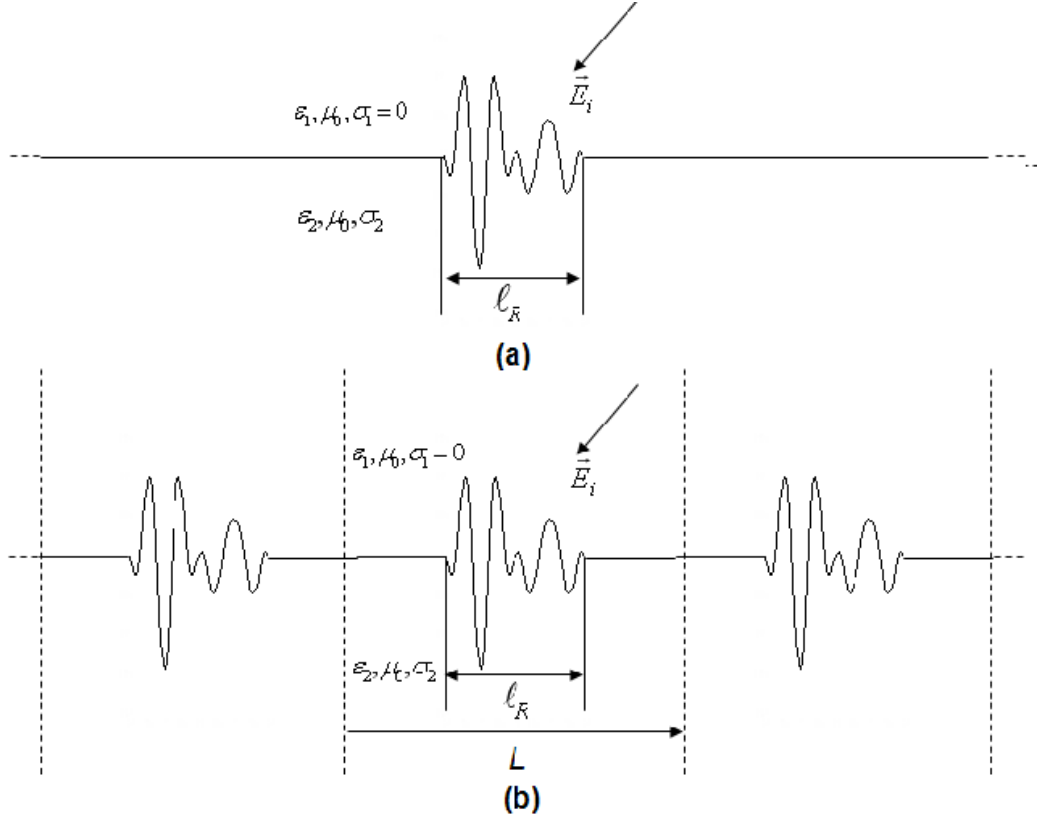


**Figure 5.9:** (a) A locally rough surface interface of infinite extent (b) its periodic model

The results of periodic model are given for  $L = 60\lambda$ . Note that the chosen period  $L = 60\lambda$  is 15 times greater than the length of the roughness  $\ell_R = 4\lambda$ . The incidence direction is  $\phi_0 = \pi/2$ , the truncation number of the series for the periodic Green's function is  $P = 90$ . The dielectric permittivity and conductivity of the lower medium are taken as  $\varepsilon_2 = 4.5\varepsilon_0$  and  $\sigma_2 = 10^{-4}$ . The computational times of the PBOA and BOA methods to get the results given Figure 5.10 with a Pentium 4 based computer are 35.469 seconds and 391.542 seconds, respectively.

On the other hand, the root mean square error between both methods is defined as

$$RMSE = \sqrt{\frac{1}{P} \sum_{i=1}^P |u_{PBOA}^i - u_{BOA}^i|^2} \quad (5.4)$$

where  $P$  is the number of the sample points. In Figure 5.11, the RMSE versus the length

of the period  $L$  used in the PBOA modeling is given, which shows that when the period  $L$  is chosen sufficiently large compared to  $\ell_R$ , the results are quite accurate.

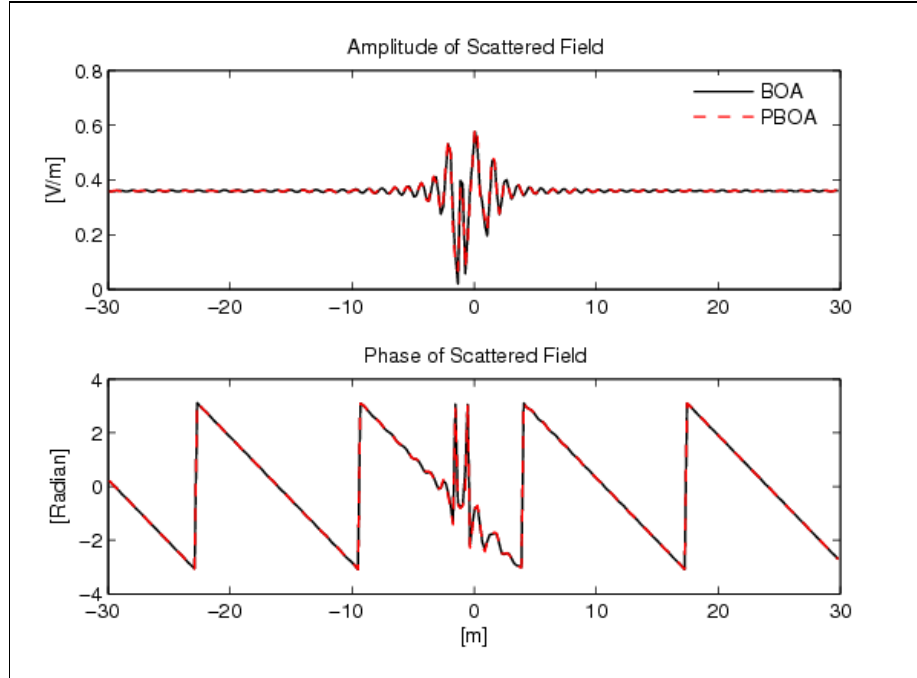


**Figure 5.10:** Comparison of the amplitude and the phase of the scattered field obtained by BOA and PBOA for a locally rough surface given in (5.3)

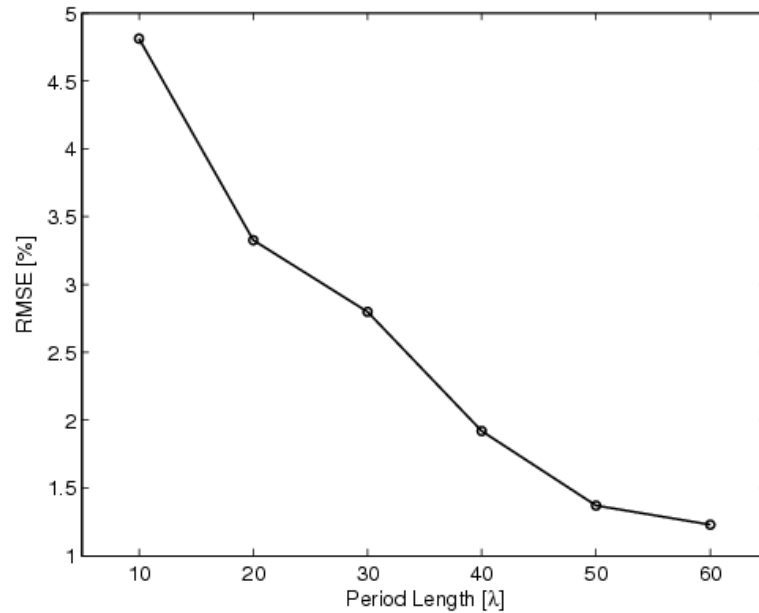


**Figure 5.11:** RMSE between BOA and PBOA for the surface given in (5.3)

Similar simulations are carried out for a random surface of rms height  $0.4\lambda$  and correlation length  $0.7\lambda$  in the case of normal incidence in which  $L = 50\lambda$  and  $P = 90$ . The electromagnetic parameters of the lower half space are selected as  $\varepsilon_2 = 8\varepsilon_0$  and  $\sigma_2 = 10^{-3}$  for this implementation. The comparisons of the amplitudes and phases of the scattered fields are shown in Figure 5.12 while the RMSE is presented in Figure 5.13. Note that the choice of period  $L$  is related to the roughness level as well as the roughness length  $\ell_R$ . It has been observed that for a surface having peak to peak variation  $0.5\lambda$  one gets good agreement in the results of both approaches for a period of  $L \approx 10\ell_R$ . For surfaces having smaller variations a  $L/\ell_R$  ratio less than 10 is sufficient.

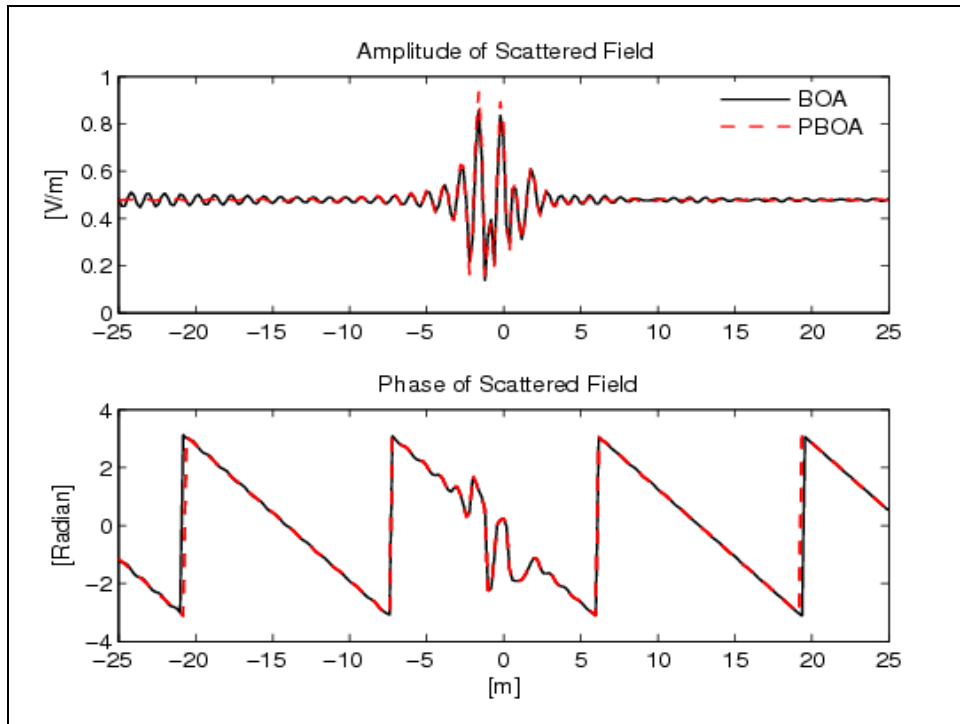


**Figure 5.12:** Comparison of the amplitude and the phase of the scattered field obtained by BOA and PBOA methods for a random surface of  $h = 0.4\lambda$ ,  $\ell = 0.7\lambda$  and  $\ell_R = 4\lambda$

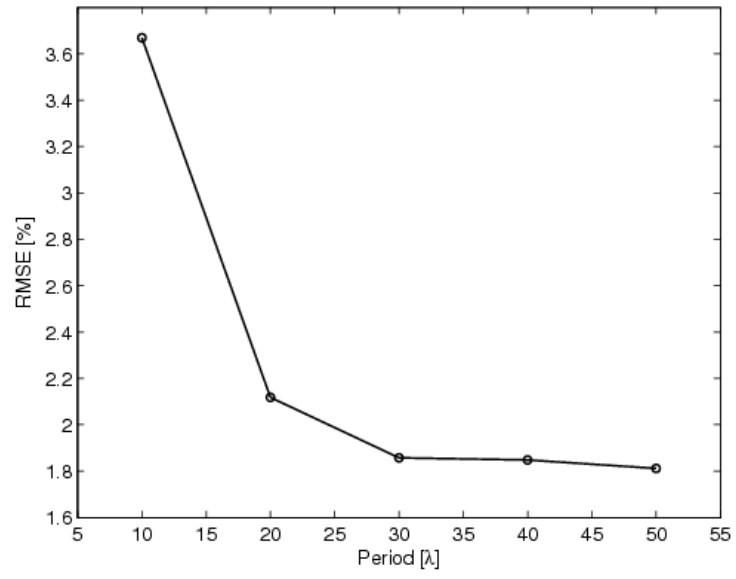


**Figure 5.13:** RMSE between BOA and PBOA for a random surface of  $h = 0.4\lambda$ ,  
 $\ell = 0.7\lambda$  and  $\ell_R = 4\lambda$



## 6. CONCLUSION

The problem of scattering of electromagnetic waves from periodic rough interfaces is solved by extending the BOA. One of the main advantages of the method is that it can also be used for the scattering from rough surfaces of infinite extend. Since the periodic Green's function of the two half-spaces media can be calculated in a pretty fast and efficient way, the computational cost of the method is cheap compared to original form of the BOA. The method yields quite accurate results for highly rough surfaces beyond the Rayleigh Hypothesis. It should be noted that in the direct and inverse scattering problems related to the objects buried in a layered media with periodic rough interfaces the determination of the periodic Green's function of the background medium constitutes a very important problem. Along this line the proposed method would be a very efficient tool to this aim by just taking the incident field as a line source. Future studies are devoted to extend the method to  $2D$  surfaces.

## REFERENCES

- [1] **Chu, H.C., Jeng, S.K. and Chen, H.C.**, 1996. Reflection and transmission characteristics of lossy periodic composite structures, *IEEE Trans. Antennas Propagat.*, **44**, 580-587.
- [2] **Butler J.K., Ferguson W. E., Evans, G.A., Stabile P.J. and Rosen, A.** 1992. A boundary element technique applied to the analysis of waveguides with periodic surface Corrugations, *Journal of the Optical IEEE Journal of Quantum Electronics*, **28**, 1701-1709.
- [3] **Janaswamy, R.**, 1992. Oblique scattering from lossy periodic surfaces with application to anechoic chamber absorbers, *IEEE Trans. Antennas Propagat.*, **40**, 162-169.
- [4] **Yang, H.Y.D. and Wang, J.**, 2001. Surface waves of printed antennas on planar artificial periodic dielectric structures, *IEEE Trans. Antennas Propagat.*, **49**, 444-450.
- [5] **Boag, A., Leviatan, Y. and Boag, A.**, 1989. Analysis of two-dimensional electromagnetic scattering from nonplanar periodic surface using a strip current model, *IEEE Trans. Antennas Propagat.*, **37**, 1437-1446
- [6] **Elachi, C.**, 1976. Waves in Active and Passive Periodic Structures: A Review, *Proceedings of IEEE* , **64**, 1666-1698
- [7] **Ulaby, F.T., Kouyate, F., Fung, A.K. and Sieber, A.J.**, 1982. A backscatterer model for a randomly perturbed periodic surface, *IEEE Trans. Geosci. Remote Sensing*, **GE-20**, 518-528.
- [8] **Purcell, A.**, 1998. The Rayleigh equations for a mutli-sinusoidal periodic surface, *J.Acoust.Soc.Am.*, **103**, 683-694.
- [9] **Chen, R. and West, J.C.**, 1996. Analysis of scattering from rough surfaces at large incidence angles using a periodic-surface Moment Method', *IEEE Trans. Geosci. Remote Sensing*, **33**, 1206-1213.

- [10] **Ikuno, H. and Yasuura, K.** 1973. Improved point-matching method with application to scattering from periodic surface, *IEEE Trans. Antennas Propagat.*, **21**, 657-662.
- [11] **Chuang, S.L. and Kong, J.A.**, 1981. Scattering of waves from periodic surfaces, *Proceeding of the IEEE*, **69**, 1232-1144.
- [12] **Plumey, J.P., Granet, G. and Chandezon, J.**, 1995. Differential covariant formalism for solving Maxwell's equations in curvilinear coordinates: Oblique scattering from lossy periodic surfaces, *IEEE Transa. Antennas Propagat.*, **43**, 835-842.
- [13]. **Wan C. and Encinar, J.A.**, 1995. Efficient computation of generalized scattering matrix for analyzing multilayered periodic structures, *IEEE Trans. Antennas Propagat.*, **43**, 1233-1242.
- [14] **Millar, R.F.**, 1973. The Rayleigh hypothesis and related least-squares solution to scattering problems for periodic surfaces and other scatterers ", *Radio Sci.*, **8**, 785-796.
- [15] **Van Den Berg P.M. and Fokkemo, J.R.**, 1980. The Rayleigh hypothesis in theory of reflection by grating, *J.Opt.Soc.Amer.*, **68**, 27-31.
- [16] **Franceschetti, G. Iodice, A. Riccio D. and Ruello, G.**, 2002. Fractal surfaces and electromagnetic extended boundary conditions, *IEEE Trans. Geosci. Remote Sensing*, **40**, 1018-1031.
- [17] **Ishimaru, A.**, 1991. *Electromagnetic Wave Propagation, Radiation and Scattering*, Prentice Hall, New Jersey.
- [18] **Altuncu, Y. , Yapar A. and Akduman I.**, 2007. Buried object approach for solving scattering problems related to rough surfaces, *Can. J. Phys.*, **85**, 39-55
- [19] **Altuncu, Y. , Yapar A. and Akduman I.**, 2006. On the Scattering of electromagnetic waves by bodies buried in a half-space with locally rough interface" *IEEE Trans. Geosci. Remote Sensing*, **44**, 1435–1443
- [20] **Altuncu, Y. , Yapar A. and Akduman I.**, 2007. Numerical computation of the Green's function of a layered media with rough interface, *Microwave Optical Tech. Letters*, **49**, 1204-1209.

- [21] **Shubair R.M. and Chow, Y.L.**, 1993. Efficient computation of the periodic Green's function in layered dielectric media, *IEEE Trans. Microwave Theory Tech.*, **41**, 498-502.
- [22] **Wallinga, G.S., Rothwell, E.J., Chen K.M. and Nyquist, D.P.**, 1999. Efficient computation of the two-dimensional periodic Green's function, *IEEE Trans. Antennas Propagat.*, **47**, 895-897.
- [23] **Nehari, Z.**, 1975. Conformal Mapping, Dover, New York, 1975.
- [24] **Petit, R.**, 1980. Electromagnetic Theory of Grating, Springer-Verlag, Germany,
- [25] **Rayleigh, L.**, 1907. On the dynamical theory of gratings, *Proc. Royal Soc.*, **79**, 399-416.
- [26] **Harrington, R.F.**, 1968. Field Computation by Moment Methods, Macmillan, Newyork.
- [27]. **Richmond, J.A.**, 1965., Scattering by dielectric cylinder of arbitrary cross section shape, *IEEE Trans. Antennas Propagat.*, **13**, 334-341.
- [28]. **Rice, S.O.**, 1951. Reflection of electromagnetic waves from slightly rough surfaces, *Commun.Pure Appl.Math.*, **4**, 351-378.

## **BIOGRAPHY**

Selda Yıldız was born in Kars, Turkey in 1983. She received her B.Sc. degree at Telecommunication Engineering at Istanbul Technical University (ITU) in 2006. After having graduated, she started her M.Sc. degree at the same department of ITU. Currently, she is working as a project assistant under supervision of Prof. Ibrahim Akduman within Electromagnetics Research Group at ITU.

## **Publications**

### **Journal Papers**

- Yıldız S., Altuncu Y., Yapar A., and Akduman I., “On the Scattering of Electromagnetic Waves by Periodic Rough Dielectric Surfaces: A BOA Solution”, IEEE Geoscience and Remote Sensing Letters (*to be published*)
- Mudanyalı O., Yıldız S., Semerci O., Yapar A., and Akduman I., "A Microwave Tomographic Approach for Non-destructive Testing of Dielectric Coated Metallic Surfaces", IEEE Geoscience and Remote Sensing Letters (*to be published*)

### **Conferences**

#### **2008 – July, EUROEM - Lausanne, Switzerland**

- S. Yıldız, Y. Altuncu and O. Ozdemir., “Scattering of Electromagnetic Waves from Periodic Rough Surfaces” (*published abstract*)

#### **2008 – June, ICIPE-Dourdan, France**

- Yapar. A, Mudanyalı O., Semerci O., Yıldız S., and Tasdemir C., " Non-Destructive Testing of Defects on Dielectric Layers" (*published paper*)

#### **2007 – August, PIERS- Prague, Czech Republic**

- Yıldız S., Altuncu Y., and Akleman F., “An Effective Method for the Scattering Electromagnetic Waves by Periodic Rough Surfaces” (*published abstract*)

#### **2007 –March, PIERS- Beijing,China**

- Mudanyalı O.,Yıldız S., and Semerci O., "Reconstruction of Perfectly Conducting Rough Surfaces Beyond a Layered Media" (*published abstract*)